A Letters Journal Exploring the Frontiers of Physics

January 2007

EPL, **77** (2007) 27007
doi: 10.1209/0295-5075/77/27007

www.epljournal.org

Optical conductivity and kinetic energy of the superconducting state: A cluster dynamical mean field study

K. Haule and G. Kotliar

Department of Physics, Rutgers University - Piscataway, NJ 08854, USA

received 26 October 2006; accepted in final form 23 November 2006
published online 18 January 2007

PACS 71.27.+a – Strongly correlated electron systems; heavy fermions
PACS 71.30.+h – Metal-insulator transitions and other electronic transitions

Abstract – We study the evolution of the optical conductivity in the t-J model with temperature and doping using the Cluster Dynamical Mean Field Method. The transition to the superconducting state in the overdoped regime is characterized by an increase in the kinetic energy of the system, in contrast to the underdoped side where kinetic energy of the system decreases upon condensation. In the underdoped and optimally doped regime, the optical conductivity displays anomalous transfers of spectral weight over a broad frequency region.

Introduction. – How superconductivity emerges from a strongly correlated normal state is one of the most important problems in the field of strongly correlated electron systems. One of the most powerful bulk probes of carrier dynamics is the optical conductivity. For example, the changes of the integral of the optical conductivity upon superfluid condensation [1,2] can be linked to the kinetic energy change, and therefore gives a direct probe of the origin of the condensation energy. Much effort was recently devoted to measure this kinetic energy difference between normal and superconducting state [3–5] using a sum rule, by integrating careful measurements of the optical conductivity up to large enough cutoff of the order of 1 eV in both normal and superconducting state. It has been shown that in the overdoped regime, the absolute value of the kinetic energy decreases, while in the underdoped regime the system *gains* kinetic energy. These surprising experimental results have been the subject of lively controversy [4,6,7] but have by now been obtained by at least three experimental groups.

It is well known that the approach to a Mott transition causes a dramatic reduction of the low energy spectral optical weight. In this paper we address the more refined issue of how the *difference* between the optical conductivity in the normal and superconducting state, and the consequent difference in kinetic energy are affected by the proximity to the Mott transition.

The optical conductivity of an electronic model governed by a Hamiltonian H consisting of a band with dispersion $\varepsilon_{\mathbf{k}}$ and gauge invariant interaction terms obeys the f-sum rule [8,9]

$$\int_0^\infty \sigma'(x)\mathrm{d}x = -\frac{\pi e^2}{4}\langle T\rangle. \tag{1}$$

The conductivity σ' is given by the current-current correlation function obtained by Peierls substitution coupling a vector potential A to the Hamiltonian $H(j=\delta H/\delta A, T=\delta^2 H/\delta A^2)$ and the bracket $\langle\cdots\rangle$ denotes the thermal average with respect to H. T is given by $T=-\sum_{\mathbf{k},\sigma,\alpha=(x,y)}[\mathrm{d}^2\varepsilon_{\mathbf{k}}/\mathrm{d}k_\alpha^2]n_{\mathbf{k}\sigma}$. In the Hubbard model $n_{\mathbf{k}}$ is the electron momentum distribution function while in the t-J model $n_{\mathbf{k}}$ is the momentum distribution of the electron operator projected to the subspace without the double occupancy.

For model lattice Hamiltonians with nearest neighbor hopping, T is the kinetic energy operator. The experimental inference of $\langle T\rangle_{super}-\langle T\rangle_{normal}$ is therefore extremely important for understanding the mechanism of high temperature superconductivity. Here $\langle T\rangle_{super}$ and $\langle T\rangle_{normal}$ are kinetic energy in superconducting and normal state, respectively. Notice that this quantity requires the evaluation of $\langle T\rangle_{normal}$ below the superconducting transition, a quantity which is well defined and can be calculated only in a mean field framework. Only mean field theory provides the possibility of defining the *continuation of the normal state* below T_c. This is the procedure done in BCS theory, and our approach represent the extensions of these ideas to correlated systems. Experimentally it is estimated by an extrapolation

procedure from the normal state data as described in ref. [7], which necessarily involves additional approximations.

In the Hubbard model, the optical conductivity has two contributions: a low energy contribution due to a motion of holes and a high energy feature at an energy scale of order U due to transitions to the upper Hubbard band involving doubly occupied sites. Hence the operator on the right hand side of eq. (1) is the sum of the two different contributions which cannot be separated. It has been shown in ref. [10] that entering the superconducting state results in a reduction of kinetic energy of the Hubbard model, in stark contrast with the BCS theory where the kinetic energy increases upon entering the superconducting state. The reduction of the kinetic energy was also found in the t-J model treated within the spin-polaron approximation [11]. Here we use the t-J model to evaluate separately the two physically different contributions, motion of holes and superexchange contribution. This allows us to make direct contact with optical experiments which measure the kinetic energy of the holes since the cutoffs which are used are such that the transitions into the upper Hubbard band, or the interband transitions, are not included.

We use the Cluster Dynamical Mean Field method on a plaquette. This approach has been used by several groups [12–18] to elucidate several qualitative aspects of the physics of the cuprates such as their phase diagram [12–14,18] and the variation of the spectral function and the electron lifetime along the Fermi surface [15–18].

We will show that this approach clearly captures the striking feature that doping induces a sign change of the difference between normal state and the superconducting state kinetic energy.

Formalism. – Our starting point is the t-J model, a lattice model consisting of two terms, a nearest neighbor hopping term t, and a nearest neighbor spin-spin antiferromagnetic exchange J. An infinite on site repulsion forbids the double occupation in any lattice site. We use an exact reformulation of this model in terms of a spin fermion model using the Hubbard-Stratonovich transformation to decouple the spin interaction. The effective action describing the interaction of fermions with spin fluctuations takes the following form:

$$S = \int_0^\beta \mathrm{d}\tau \Bigg\{ \sum_{\mathbf{k}\sigma} c^\dagger_{\mathbf{k}\sigma}(\tau) \left(\frac{\partial}{\partial\tau} - \mu + \epsilon_{\mathbf{k}} \right) c_{\mathbf{k}\sigma}(\tau) + \sum_i U n_{i\uparrow}(\tau) n_{i\downarrow}(\tau) + \sum_{\mathbf{q}} \Bigg[\mathbf{\Phi}^\dagger{}_{\mathbf{q}}(\tau) \frac{2}{J_{\mathbf{q}}} \mathbf{\Phi}_{\mathbf{q}}(\tau) + i\, \mathbf{S}_{\mathbf{q}} \left(\mathbf{\Phi}^\dagger_{\mathbf{q}}(\tau) + \mathbf{\Phi}_{-\mathbf{q}}(\tau) \right) \Bigg] \Bigg\}. \quad (2)$$

The Hubbard U term in the action will be taken to infinity to enforce the constraint. Here $\Phi_{\mathbf{q}}$ is the Hubbard-Stratonovich vector bosonic field which decouples spin-spin interaction of the J term [19], $\mathbf{S}_{\mathbf{q}}$ is the spin operator, $J_{\mathbf{q}}$ and $\epsilon_{\mathbf{k}}$ are dispersion of the spin and hopping term of the t-J model.

The exact Baym-Kadanoff functional for this problem is

$$\Gamma[\mathcal{G},\mathcal{D}] = -\mathrm{Tr}\log(G_0^{-1} - \Sigma) - \mathrm{Tr}[\mathcal{G}\Sigma] + \frac{1}{2}\mathrm{Tr}\log(\mathcal{D}_0^{-1} - \Pi) + \frac{1}{2}\mathrm{Tr}[\mathcal{D}\Pi] + \Phi[\mathcal{G},\mathcal{D}], \quad (3)$$

where $\mathcal{G}$ and Σ are the Green's function and self-energy of the electrons while $\mathcal{D}$ and Π are Green's function and self-energy of the Hubbard-Stratonovich bosonic field [19,20]. The $\Phi[\mathcal{G},\mathcal{D}]$ functional is the sum of all two particle irreducible diagrams constructed from the Green's functions and the bare interactions [21]. In eq. (3) $\mathcal{G}$ is a matrix in cluster momenta and Numbu space. The self-consistent solution selects d-wave symmetry for the anomalous components ($\mathcal{F}_{(\pi,0)} = -\mathcal{F}_{(0,\pi)}$ and zero in other patches where $\mathcal{F}$ is the anomalous Green's function).

We use the Extended Dynamical Cluster Approximation (EDCA) [12–14,22] on a plaquette because it is the simplest cluster dynamical mean field method that justifies ignoring the vertex corrections of optical conductivity and has the advantage of describing better the spin fluctuations by allowing the cluster spin to relax more efficiently through its direct exchange interaction with the bath. The only approximation of the EDCA is to replace the Green's functions in the interacting part of the functional $\Phi[\mathcal{G},\mathcal{D}]$ with the corresponding course grained cluster Green's functions $\mathcal{G}_{\mathbf{k}} \to \mathcal{G}_{\mathbf{K}} = \sum_{\mathbf{k}\in\mathbf{K}} G_{\mathbf{k}}$ and $\mathcal{D}_{\mathbf{q}} \to \mathcal{D}_{\mathbf{Q}} = \sum_{\mathbf{q}\in\mathbf{Q}} \mathcal{D}_{\mathbf{Q}}$ where the sum $\sum_{\mathbf{k}\in\mathbf{K}}$ is over those $\mathbf{k}$ momenta in Brillouin zone which correspond to certain cluster momenta $\mathbf{K}$ (see [12]). The saddle point equations of the functional eq. (3) are $\Sigma_{\mathbf{K}} = \delta\Phi/\delta\mathcal{G}_{\mathbf{K}}$ and $\Pi_{\mathbf{Q}} = 2\delta\Phi/\delta\mathcal{D}_{\mathbf{Q}}$ which automatically give piecewise constant self-energies. Together with the Dyson equations $\mathcal{G}_{\mathbf{K}} = \sum_{\mathbf{k}\in\mathbf{K}}(G_0^{-1} - \Sigma_{\mathbf{K}})^{-1}$ and $\mathcal{D}_{\mathbf{Q}} = \sum_{\mathbf{q}\in\mathbf{Q}}(D_0^{-1} - \Pi_{\mathbf{Q}})^{-1}$ form a closed set of equations. Few comments are in order: i) The bosonic self-energy is simply related to the spin susceptibility [20] $\chi_{\mathbf{q}} = (g^2\Pi_{\mathbf{Q}}^{-1} + J_{\mathbf{q}})^{-1}$ and this expression can be used to calculate bosonic self-energy knowing local spin-susceptibility. ii) The Baym-Kadanoff functional $\Phi[\mathcal{G},\mathcal{D}]$ which depends only on the cluster Green's functions can be obtained by solving the cluster problem coupled to the fermionic and bosonic bath [14,22]. As an impurity solver we use the exact diagonalization for the cluster and an NCA approach to treat the hybridization of the cluster with the bath. This method, allows us to access only the temperatures not much lower than the critical temperature (of the order of $0.8\,T_c$).

Within DCA, the vertex corrections to the conductivity vanish just like in single site DMFT. This is because diagrams involving vertex corrections carry a factor $\sum_{\mathbf{k}\in\mathbf{K}} v_{\mathbf{k}} \mathcal{G}_{\mathbf{k}} * \mathcal{G}_{\mathbf{k}}$ where $\mathbf{K}$ is the patch in momentum space labeled by cluster momenta $\mathbf{K}$. In the 2×2 plaquette, *all* the patches are symmetric under $\mathbf{k} \to -\mathbf{k}$ and the

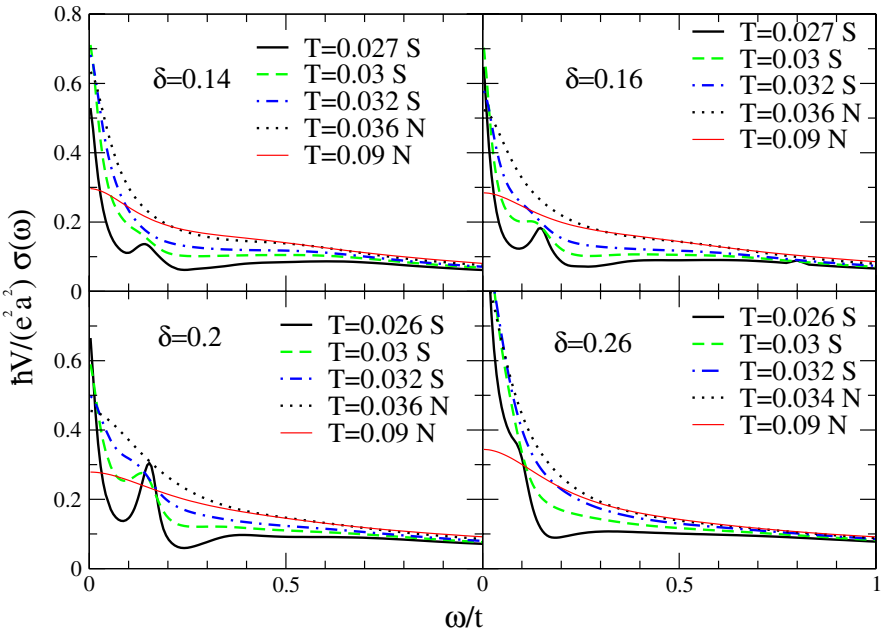

Fig. 1: Optical conductivity across the superconducting transition for various doping levels from underdoped to overdoped regime. Letter S in legend stands for superconducting state and N for normal state of the t-J model.

integral vanishes. The optical conductivity can therefore be simply expressed by

$$\sigma'(\omega) = \sum_{\mathbf{k}\sigma} e^2 v_{\mathbf{k}}^2 \int \frac{\mathrm{d}x}{\pi} \frac{f(x-\omega)-f(x)}{\omega} \times [\mathcal{G}''_{\mathbf{k}}(x-\omega)\mathcal{G}''_{\mathbf{k}}(x) + \mathcal{F}''_{\mathbf{k}}(x-\omega)\mathcal{F}''_{\mathbf{k}}(x)] , \quad (4)$$

where $v_{\mathbf{k}}$ is electron bare velocity, $\mathcal{G}_{\mathbf{k}}$ and $\mathcal{F}_{\mathbf{k}}$ are the normal and anomalous Green's functions, respectively. To study superconductivity we allow the off-diagonal long range order by employing the Nambu formalism.

Results. – In the following we describe our results in the light of the current experimental situation. Given the simplicity of the model used, and the fact that experiments probe the kinetic energy change at a temperature of the order of $0.1\,T_c$, we stress the qualitative rather than quantitative results of our work.

Throughout the paper we use $J/t = 0.3$ and $t = 1$. In fig. 1 we show the evolution of the optical conductivity for various temperatures and dopings from room temperature $T \approx 0.09t$ down to transition temperature $T_c \approx 0.034t$ and slightly below the transition $T \approx 0.76T_c$. We have representatives of the three regimes of the cuprate superconductors, slightly underdoped $\delta = 0.14$, optimally doped $\delta = 0.16$–0.2 and the overdoped case $\delta = 0.26$. In agreement with earlier theoretical single site DMFT studies [23,24], the optical conductivity extends over a broad frequency range, and consists of a broad Drude component at low frequencies that sharpens with decreasing temperature and a higher frequency ("mid infrared") component with substantial intensity at high frequencies.

Upon entering the superconducting state no real optical gap opens below the transition, unlike the standard case of the s-wave BCS superconductors. However, a substantial reduction of the optical conductivity due to superconductivity is observed up to very high frequency even beyond $\omega > t \approx 2500\,\mathrm{cm}^{-1}$ which is ten times bigger that the superconducting gap at optimal doping $\Delta \approx 0.1t$ itself.

The Drude-like low frequency conductivity narrows as the temperature decreases from room temperature to just above T_c and continues to grow even below the transition temperature. This enhancement of the low frequency conductivity as a result of the onset of coherence is seen in many experimental studies [25] and should be contrasted with the reduction of the conductivity at higher frequencies due to the opening of a gap.

The optical conductivity has a very long tail of incoherent spectral weight that dominates the optics. Furthermore, the tail seems to have an approximate power law $\sigma \propto (-i\omega)^{\alpha}$ with the exponent close to $\alpha = 2/3$ [26]. At low frequency, optical conductivity is Lorentzian-like at optimal doping with ω/T scaling. In fig. 2b we plot $(T\sigma(\omega))^{-1}$ as a function of ω/T which is temperature independent quadratic parabola in the region $-T \lesssim \omega \lesssim T$. Similar behavior was noticed in ref. [27].

We also point out some quantitative discrepancy between the present cluster DMFT study of the t-J model and experiments on cuprates. In our calculation, the location of the optimal doping is shifted to slightly higher doping levels ($\sim 18\%$) and the superconducting dome is flatter than observed experimentally. Finally, the peak in optical conductivity around $0.15t$ is the standard BCS coherence peak arising from the excitations

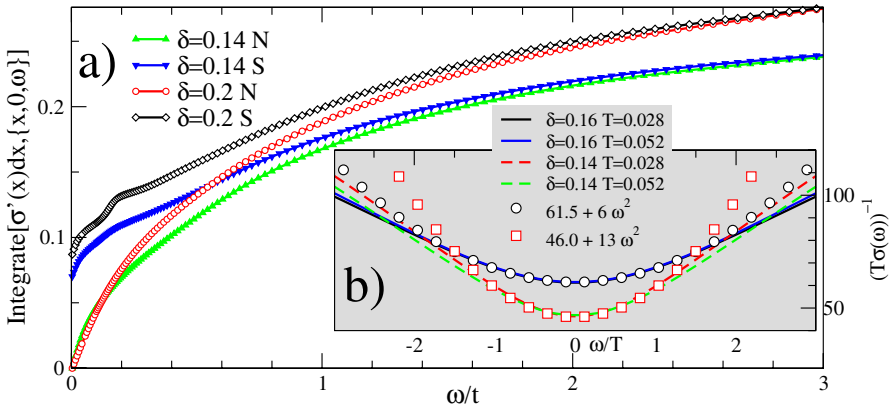

Fig. 2: a) The integral of the optical conductivity $\int_0^\omega \sigma'(x)\mathrm{d}x$ for normal and superconducting state at $T = 0.028t$. The optical weight in SC state missing in the finite frequency region collapses into a δ function. The spectral weight is restored when the integral is taken up to $\sim 4t \sim 1\,\mathrm{eV} \approx 8000\,\mathrm{cm}^{-1}$. b) The inverse of low frequency optical conductivity $1/(T\sigma(\omega))$ *vs.* ω/T is a quadratic parabola independent of temperature in the optimal doping regime. Optical conductivity is thus Drude-like at low frequency up to $\omega \sim T$.

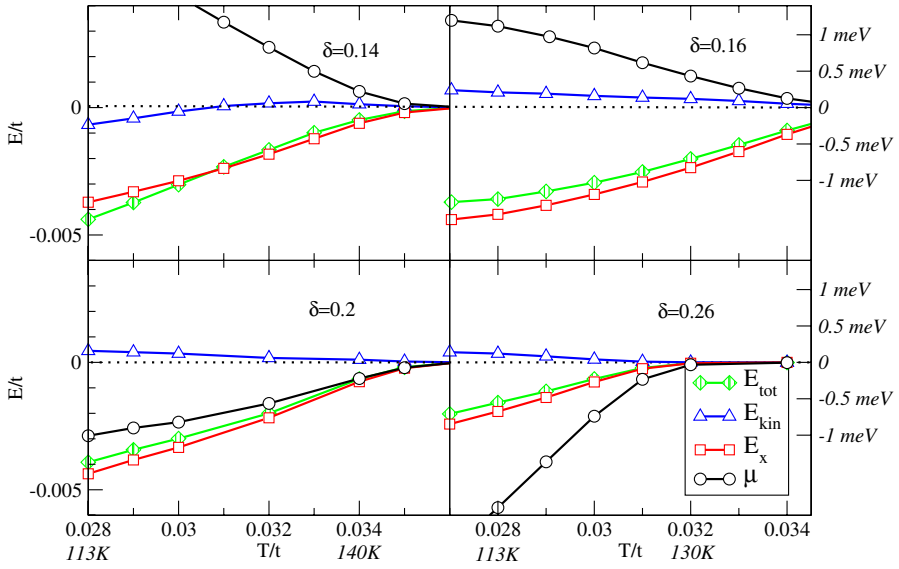

Fig. 3: (Color online) The difference between the superconducting and normal state energies as a function of temperature. The following curves are shown: blue with triangles up - $E_{kin-S} - E_{kin-N}$; red squares - $E_{exch-S} - E_{exch-N}$; green diamonds - $E_{tot-S} - E_{tot-N}$; black with circles - $\mu_S - \mu_N$. The meV units on the left side were obtained using the usual value for $t \sim 400\,\mathrm{K} \sim 0.35\,\mathrm{eV}$.

across the superconducting gap in one particle density of state and is not visible in experiment which is closer to the clean limit than our theoretical calculation which overestimates the scattering rate.

Transfer of spectral weight. – A surprising aspect of the physics of strongly correlated materials, is that low energy phenomena affect the spectra of the material over a very large energy scale. This general phenomena is illustrated in fig. 2a, which shows the integral of optical spectral weight in the normal and the superconducting state. Low energy phenomena like the onset of superconductivity which involves a scale of a fraction of J, involve redistribution of optical weight of the order of $4t \approx 1\,\mathrm{eV}$ which is 40 times more than the gap value. A theoretical insight from our calculation is that the high frequency redistribution of weight comes from the anomalous Greens function $\mathcal{F} * \mathcal{F}$ in eq. (4) and hence cannot be observed in the density of states or ARPES measurements. The large range of redistribution of spectral weight was also measured on cuprates and pointed out in [2,4]; however, in experiments the redistribution of spectral weight drops very fast with doping and in the slightly overdoped regime, the spectral weight might be recovered even in the conventional range. In our calculation, the redistribution of weight decreases on overdoped site as well, but the rate of the change is slower than measured in cuprates.

In fig. 3, we show the change of kinetic energy of holes, the superexchange energy $(\sum_{ij} J_{ij}\langle \mathbf{S}_i \mathbf{S}_j \rangle/2)$ and

total energy upon condensation as obtained from our cluster DMFT calculation. The kinetic energy can be directly calculated from the spectral function and the superexchange energy from the spin susceptibility. Most of the condensation energy arises from an increase in magnitude of the spin-spin correlations $\langle \mathbf{S}_i \mathbf{S}_j \rangle$ when entering the superconducting state in agreement with strong coupling [28] and weak coupling [29] analysis.

In agreement with very recent experiments on cuprates [3], we see that the change in kinetic energy upon superfluid condensation reverses sign between overdoped to underdoped regime. In overdoped regime, the conventional BCS picture is applicable where kinetic energy of the system increases while the superexchange energy decreases just like the interaction energy in conventional phonon mediated superconductors. The later difference is much larger such that the total condensation energy is positive. In underdoped regime, the superexchange energy still decreases upon condensation and gives the largest contribution to the condensation energy [14]. However, the kinetic energy of holes is gained in the underdoped case so that the kinetic energy contributes to the condensation energy gain.

In fig. 3, we also show the change of chemical potential upon condensation. Similarly to kinetic energy, it also changes sign with doping and it increases in the underdoped regime while it decreases in the overdoped regime. This is a consequence of the asymmetry of the normal as well as the superconducting one particle density of states.

While the vertex corrections vanish in the simplest mean field cluster approach (EDCA on a plaquette), they are nonzero in the real space cluster schemes, Cellular-DMFT [30] on the plaquette. By computing kinetic energy directly from the one-particle Green's function in Cellular-DMFT, the short range vertex corrections are fully taken into account. We have checked that all our qualitative results are captured also in Cellular-DMFT, where the cumulant periodization [31] is necessary to capture the Fermi surface shrinking and correct kinetic energy change from underdoped to overdoped regime.

In conclusion, we have studied the t-J model at finite temperatures using the cluster DMFT on a plaquette near the optimally doped regime where the maximum of the superconducting temperature is located. The mean field theory captures the main qualitative features of the transition from the overdoped to underdoped regime and how it effects the delicate balance of kinetic and exchange energy between the normal and superconducting state.

* * *

We are grateful to N. Bontemps, A. Georges and P. Wölfle for useful discussions. GK was supported by NSF DMR Grant No. 0528969.

REFERENCES

[1] Ferrell R. A. and Glover R. E., *Phys. Rev.*, **109** (1958) 1398; Tinkham M. and Ferrell R. A., *Phys. Rev. Lett.*, **2** (1959) 331.
[2] Santander-Syro A. F., Lobo R. P. S. M. and Bontemps N., *Phys. Rev. B*, **70** (2004) 134504; Santander-Syro A. F., Lobo R. P. S. M. and Bontemps N., cond-mat/0404290.
[3] Deutscher G., Santander-Syro A. F. and Bontemps N., *Phys. Rev. B*, **72** (2005) 092504.
[4] Molegraaf H. J. A., Presura C., van der Marel D., Kes P. H. and Li M., *Science*, **295** (2002) 2239.
[5] Hwang J., Timusk T. and Gu G. D., cont-mat/0607653.
[6] Boris A. V., Kovaleva N. N., Dolgov O. V., Holden T., Lin C. T., Keimer B. and Bernhard C., *Science*, **304** (2004) 708; Santander-Syro A. F. and Bontemps N., cond-mat/0503767.
[7] Kuzmenko A. B., Molegraaf H. J. A., Carbone F. and van der Marel D., cond-mat/0503768.
[8] Kubo R., *J. Phys. Soc. Jpn.*, **12** (1957) 570.
[9] Maldague P. F., *Phys. Rev. B*, **16** (1977) 2437.
[10] Maier Th. A., Jarrell M., Macridin A. and Slezak C., *Phys. Rev. Lett.*, **92** (2004) 27005.
[11] Wrobel P., Eder R. and Fulde P., *J. Phys. Condens. Matter*, **15** (2003) 6599.
[12] Maier T., Jarrell M., Pruschke T. and Hettler M. H., *Rev. Mod. Phys.*, **77** (2005) 1027.
[13] Hettler M. H., Tahvildar-Zadeh A. N., Jarrell M., Pruschke T. and Krishnamurthy H. R., *Phys. Rev. B*, **58** (1998) R7475.
[14] Maier Th. A., *Physica B: Condens. Matter*, **359-361** (2005) 512; Maier Th. A., cond-mat/0312447.
[15] Civelli M., Capone M., Kancharla S. S., Parcollet O. and Kotliar G., *Phys. Rev. Lett.*, **95** (2005) 106402.
[16] Parcollet O., Biroli G. and Kotliar G., *Phys. Rev. Lett.*, **92** (2004) 226402.
[17] Kancharla S. S., Civelli M., Capone M., Kyung B., Senechal D., Kotliar G. and Tremblay A.-M. S., cond-mat/0508205.
[18] Kyung B., Georges A. and Tremblay A.-M. S., *Phys. Rev. B*, **74** (2006) 024501; Kyung B., Kotliar G. and Tremblay A.-M. S., *Phys. Rev. B*, **73** (2006) 205106; Kyung B., Kancharla S. S., Senechal D., Tremblay A.-M. S., Civelli M. and Kotliar G., *Phys. Rev. B*, **73** (2006) 165114.
[19] Smith J. L. and Si Q., *Phys. Rev. B*, **61** (2000) 5184; Si Q., Rabello S., Ingersent K. and Smith J. L., *Phys. Rev. B*, **68** (2003) 115103.
[20] Haule K., Ph D Thesis, University of Ljubljana (2002) (`http://morje.ijs.si/haule/thesis/html/`).
[21] Kotliar G., Savrasov S. Y., Haule K., Oudovenko V. S., Parcollet O. and Marianetti C. A., cond-mat/0511085.
[22] Haule K., Rosch A., Kroha J. and Wölfle P., *Phys. Rev. Lett.*, **89** (2002) 236402; *Phys. Rev. B*, **68** (2001) 155119.
[23] Jarrell M. and Freericks J. K., *Th. Pruschke Phys. Rev. B*, **51** (1995) 11704.
[24] Toschi A., Capone M., Ortolani M., Calvani P., Lupi S. and Castellani C., *Phys. Rev. Lett.*, **95** (2005) 097002.

[25] Lee Y. S., Segawa K., Li Z. Q., Padilla W. J., Dumm M., Dordevic S. V., Homes C. C., Ando Y. and Basov D. N., *Phys. Rev. B*, **72** (2005) 054529; Homes C. C., Dordevic S. V., Bonn D. A., Liang R. and Hardy W. N., *Phys. Rev. B*, **69** (2003) 24514.
[26] Haule K. and Kotliar G., cond-mat/0605149.
[27] van der Marel D., Molegraaf H. J. A., Zaanen J., Nussinov Z., Carbone F., Damascelli A., Eisaki H., Greven M., Kes P. H. and Li M., *Nature*, **425** (2003) 271.
[28] Kotliar G. and Liu J., *Phys. Rev. B*, **38** (1988) 5142.
[29] Scalapino D. J. and White S. R., *Phys. Rev. B*, **58** (1998) 8222.
[30] Kotliar G., Savrasov S. Y., Palsson G. and Biroli G., *Phys. Rev. Lett.*, **87** (2001) 186401.
[31] Stanescu T. D. and Kotliar G., *Phys. Rev. B*, **74** (2006) 125110.